ELSEVIER

Journal of Nuclear Materials 246 (1997) 206–214

journal of nuclear materials

Contribution of recoil atoms to irradiation damage in absorber materials

D. Simeone [a,*], O. Hablot [a], V. Micalet [a], P. Bellon [b], Y. Serruys [b]

[a] *Centre d'Etudes de Saclay, Laboratoire d'Etudes des Matériaux Absorbants, F-91191 Gif-sur-Yvette cedex, France*
[b] *Centre d'études de Saclay, Service de Recherches de Métallurgie Physique, F-91191 Gif-sur-Yvette cedex, France*

Received 29 January 1997; accepted 15 April 1997

Abstract

Absorbing materials are used to control the reactivity of nuclear reactors by taking advantage of nuclear reactions (e.g., $^{10}B(n,\alpha)^{7}Li$) where neutrons are absorbed. During such reactions, energetic recoils are produced. As a result, radiation damage in absorbing materials originates both from these nuclear reactions and from elastic collisions between neutrons and atoms. This damage eventually leads to a partial destruction of the materials, and this is the main limitation on their lifetime in nuclear reactors. Using a formalism developed to calculate displacements per atoms (dpa) in a multi atomic target, we have calculated damages in terms of displacements per atom in a (n,α) absorbing material taking into account geometrical effects of 10 boron self shielding and transmutation reactions induced by neutrons inside the absorber. Radiation damage is calculated for boron carbide and hafnium diboride ceramics in a Pressurized Water Reactor environment. It is shown that recoils produced by nuclear reactions account for the main part of the radiation damage created in these ceramics. Damages are calculated as a function of the distance from the center of an absorber pellet. Due to the self-shielding effect, these damage curves exhibit sharp maxima, the position of which changes in time. © 1997 Elsevier Science B.V.

1. Introduction

Control rods of pressurized water reactors (PWR) are used to control generating plants. These control pins are made of two kinds of absorbers, an alloy of silver, indium and cadmium, and ceramic materials containing boron, such as boron carbides. ^{10}B can efficiently absorb low and fast neutrons. That is why boron carbide is used in fast breeder reactors (FBR) and in PWRs. With the new generation of PWRs, absorber pins will have to be able to capture more neutrons. Hafnium diboride could be an attractive material for this kind of reactors, because of the high neutron absorption cross-section of both hafnium and 10 boron. In addition, their low cost of fabrication, their high melting point ($T_m = 2400°C$ for B_4C, and $T_m = 3380°C$ for HfB_2), and their low neutron activity, make them attractive materials for the nuclear industry. The evolution of such materials under irradiation is however not well understood. It is observed that after a typical burnup of 5%, B_4C pellets fall apart [1]. The most likely explanation proposed so far is that this destruction comes purely from the high stresses built up by lenticular He bubbles [1]. Indeed, in the $^{10}B(n,\alpha)^{7}Li$ nuclear reaction, neutrons with a kinetic energy of about 25 meV and above are absorbed, which generates helium and lithium atoms. However, radiation damages may play a role in this degradation process, and so far there has been very few calculations of radiation damages in materials undergoing nuclear reactions [2]. In such materials, in addition to the damage produced by elastic collisions between neutrons and target atoms, energetic recoils are a second source of damage: indeed the $^{10}B(n,\alpha)^{7}Li$ reaction generates helium and lithium atoms with an average kinetic energy of 1.48 and 0.83 MeV, respectively. Moreover, the high thermal neutron absorbing cross-section of ^{10}B induces non-uniform production profiles of lithium and helium atoms in the absorbing pellets. These profiles lead to a non-uniform

* Corresponding author. Tel.: +33-1 69 08 29 20; fax: +33-1 69 08 90 82; e-mail: lema@semt.smts.cea.fr.

PII S0022-3115(97)00092-5

damage rate in these absorbers. Here, we present calculations of damages, taking into account the role of recoil atoms and the chemistry shift induced by lithium and helium atom formation and geometric effects due to self shielding of 10 boron atoms in such absorbers. This paper is divided into three parts: the formalization of the damage calculation in a polyatomic material, the calculation damages in boron carbide and in hafnium diboride, and the computation of the damages profile along the radius of such neutron absorbing pellets.

2. Displacement cross-section calculation

A Binary Collision Approximation (BCA) model will be used in this paper to calculate the average number of displaced atoms induced by a neutron irradiation. This model is also applicable to ion or electron irradiations. The BCA method requires only interaction potentials for close approaches between atoms. The crystalline structure of the target will not be taken into account. Such a framework has been extensively used for calculating radiation damage due to charged particles [3,4]. Atomistic computer simulations performed in the last decade [5,6] have shown that this results in an overestimation of the number of displaced atoms during the irradiation. However, any real improvement of the calculations presented below would require the development of realistic interatomic potentials stabilizing the complex crystal structures of absorbing materials (the unit cell of boron carbide is rhombohedral with icosahedral units at the corners, and a three atoms chain along the main diagonal; the unit cell of hafnium diboride is an hexagon composed of intercalated plans of boron and hafnium). This task is beyond the scope of this paper.

As recalled above, collisions of recoil atoms with target atoms have to be treated to calculate damages in absorber materials. For this purpose, we have developed a specific code, DIANE (displacement induced by irradiation of atoms by ions and neutrons and electrons), based on a formalism introduced by Albermann and Lesueur [2] for handling multicomponent targets. Moreover, displacement threshold energies are allowed to take different values for each species. As an example of application, displacements per atom have been calculated for boron carbide and hafnium diboride irradiated by a typical PWR neutron flux spectrum.

2.1. Presentation of the formalism

Three hypotheses have been used to calculate the number of displaced atoms during an irradiation:

H1: The collision process can be treated as a binary encounter.

H2: The crystal is considered as an amorphous material. Neither canalization nor focalization effects are taken into account. The target atoms are randomly distributed.

H3: The thickness of the crystal is higher than the projectile mean free path. Therefore, the stopping power can be considered as a continuous function of the penetration distance of the projectile into the target.

2.1.1. Equations of the problem

The first step in producing damage calculations is the estimation of the number of primary knocked atoms (PKA) by the elastic scattering of incident ions, electrons or neutrons. This step is treated by using universal cross-sections derived by Lindhart et al. [7], using a Thomas Fermi model for ions, and hard sphere cross-sections for neutrons.

The second step is the production of cascades created by each PKA. The PKA dissipates its initial energy in two ways. Some energy is lost by exciting the electrons of the medium or those of the PKA itself. The PKA has elastic collisions with atoms of the target. To calculate the number of atoms displaced by cascades, we formulate the problem in terms of integral equations in the manner presented by Lindhart et al. [7]. The basic idea of this formalism is that the sum of the number of displaced atoms induced by a particle participating in a specific collision process should be conserved before and after that collision.

Neglecting displacement induced by electrons because of their low momentum, the balance of the number of displaced atoms, $n(E)$, created by the PKA of energy E yields in a slide $\mathrm{d}x$ of mono-atomic target:

$$n(E) = N\,\mathrm{d}x\left(\int \mathrm{d}\sigma_{\mathrm{n,e}}\left(n\left(E - T_{\mathrm{a}} - \sum_i T_{ei}\right) + n(T_{\mathrm{a}} - U_{\mathrm{a}})\right)\mathrm{d}T\right) + \left(1 - N\,\mathrm{d}x\int \mathrm{d}\sigma_{\mathrm{n,e}}\right)n(E), \tag{1}$$

where N is the number of atoms per volume unit, $\mathrm{d}x$ the length of the slide, $\mathrm{d}\sigma_{\mathrm{n,e}}$ the differential cross-section of the projectile with a nucleus of the target or with an electron of the target atom, U_{a} the energy wasted to break the atomic binding of a target atom, T_{ei} the energy transferred to the ith electron of the target atom, and T_{a} the energy transferred to the mass center of the struck atom.

Lesueur has shown that, under the assumptions of Lindhart et al. [7], for a polyatomic target composed of p elements, Eq. (1) is replaced by a set of $(p+1)$ equations that can be written as

$$S_0(E)\frac{\mathrm{d}n_{0j}}{\mathrm{d}E}(E) - \left(c_j\int P_j(T)\frac{\mathrm{d}\sigma_{0j}}{\mathrm{d}T}(E,T)\,\mathrm{d}T + \sum_{i=1}^{p} c_i\int \frac{\mathrm{d}\sigma_{0i}}{\mathrm{d}T}n_{ij}(T)\,\mathrm{d}T\right) = 0, \tag{2}$$

where $S_0(E) = \sum_{i=1}^{p} c_i(S_{0i}^n(E) + S_{0i}^e(E))$ is the total stopping power for the projectile, called 0 and hereafter re-

ferred to by using subscript 0, $S_{0i}^{e}(E)$ the electronic stopping power, and $S_{0i}^{n}(E)$ the nuclear stopping power, c_j the atomic fraction of the jth atomic species of the target, $(\mathrm{d}\sigma_{0j}/\mathrm{d}T)(E, T)$ the differential cross-section between atom 0 and atom j, T the recoil energy of atom j, $T_m = \lambda_{0j}E$ and λ_{0j} is equal to $(4M_0M_j)/(M_0 + M_j)^2$, where M_0 is the mass of the projectile and M_j is the mass of the atom j, $P_j(T)$ the probability for an atom j of the target to be displaced from its equilibrium position during a collision with another atom, and n_{ij} the number of displaced j atoms in a collision induced by atom i recoiling in the medium composed of p elements.

To obtain $n_{ij}(E)$, one should solve the set of p following integrodifferential equations:

$$S_i(E)\frac{\mathrm{d}n_{ij}}{\mathrm{d}E} - \left(c_j \int \frac{\mathrm{d}\sigma_{ij}}{\mathrm{d}T}(E, T) R_{ij}(T)\,\mathrm{d}T + \sum_{k=1}^{p} c_k \int \frac{\mathrm{d}\sigma_{ik}}{\mathrm{d}T}(E, T) n_{kj}(T)\,\mathrm{d}T \right) = 0, \tag{3}$$

with $R_{ij}(T) = P_j(T)(\delta_{ij} + (1 - \delta_{ij})P_j(E - T)$, where δ_{ij} is the Kronecker symbol. The term in brackets inside the second term of Eq. (3) takes into account replacements of an atom A inside the sub-lattice A.

The set of p equations of Eq. (3) is solved using an iterative process [2]. The final values of $n_{ij}(E)$ are injected in Eq. (2), which makes it possible to calculate $n_{0j}(E)$.

2.1.2. Scattering cross-sections and stopping powers

With the help of impulse approximations and extrapolations to large scattering angles, Lindhart et al. [7] have developed a universal function for the nuclear scattering cross-section, which is represented in terms of the dimensionless energy parameter t as

$$\frac{\mathrm{d}\sigma_{ij}^{n}}{\mathrm{d}T}(E, T)\,\mathrm{d}T = \frac{\pi a_{ij}^2}{2}\frac{f(t^{1/2})}{t^{3/2}}\mathrm{d}t,$$

where

$$t = \frac{TEM_j}{M_i}\left(\frac{a}{2Z_iZ_je^2}\right)^2$$

and a is the Lindhart screening radius:

$$a = \frac{0.8853a_0}{\left(Z_i^{2/3} + Z_j^{2/3}\right)^{1/2}},$$

where a_0 is the Bohr radius.

The nuclear stopping power is calculated by integrating over all possible values of the energy:

$$S_{ij}^{n}(E) = \int_0^{\lambda_{ij}E} T\frac{\mathrm{d}\sigma_{ij}^{n}}{\mathrm{d}T}(E, T)\,\mathrm{d}T. \tag{4}$$

The nuclear stopping power has its maximal value for about 1 keV/amu. The electronic stopping power is calculated using the Lindhart formula [8] for middle velocities (up to 25 keV/amu) and the Bethe formula [9] for higher velocities. The effective charge of the projectile in the Bethe formula is estimated by the Ziegler formula [10].

2.1.3. Probability function

E_{dj} is the threshold energy for the species j. Using the Kinchin and Pease model [11], the probability function for an atom to be displaced is written as

$$P(E) = 0 \quad \text{if } E < E_d,$$
$$P(E) = 1 \quad \text{if } E > E_d.$$

2.2. The displacement cross-section due to $^{10}B(n,\alpha)^7Li$ reactions

For absorbers containing ^{10}B, neutrons produce ^{10}B(n,α)^{7}Li reactions. The recoils of ^{4}He and ^{7}Li atoms are a new source of damage. A displacement cross-section is associated to these reactions. This displacement cross-section is the product of the probability to absorb a neutron multiplied by the number of defects produced by lithium and helium recoil atoms. The ^{10}B(n,α)^{7}Li cross-section can be described by the Breit Wigner formula [12]. The ^{10}B atom is a light atom and no resonances exist for neutron energies up to 1 MeV [13], then the ^{10}B(n,α)^{7}Li cross-section follows a classical absorption law proportional to $1/\sqrt{E}$. Between 1 and 10 MeV, the ^{10}B(n,α)^{7}Li cross-section exhibits resonances. But these resonances are smooth and in first approximation the $1/\sqrt{E}$ law can be used. Then the ^{10}B(n,α)^{7}Li cross-section can be written as

$$\sigma(E) = A\sqrt{\frac{E_0}{E}}.$$

The displacement cross-section due to the ^{10}B(n,α)^{7}Li reaction can be written as

$$\sigma^{ab}(E) = A\sqrt{\frac{E_0}{E}}\left(\sum_{i=1}^{p} n_{\mathrm{Li}i}(0.83\,\mathrm{MeV}) + n_{\mathrm{He}i}(1.48\,\mathrm{MeV}) \right), \tag{5}$$

where A is about 0.606 b and E_0 is equal to 1 MeV [13], $n_{\mathrm{Li}i}$ is the number of atoms displaced by a 0.83 MeV lithium atom, $n_{\mathrm{He}i}$ is the number of atoms displaced by a 1.48 MeV helium atom, and E is the kinetic energy of the neutron. No nuclear reaction is induced by neutrons on carbon atoms in boron carbide.

For hafnium diboride absorbers, epithermal neutrons ($E \cong 1$ eV) are absorbed and then induce a γ emission. Energies of nuclei recoiling from the emission of a γ photon [14] have been estimated in Table 1 for each hafnium isotope. These recoil energies are presented in Table 1. All these recoil energies being low, the recoils of hafnium atoms are not taken into account in our calculations.

Table 1
The hafnium isotopes emit photons when they absorb neutrons. Measuring the maximum photon energies (column 1), it is possible to calculate the kinetic energies of recoils (column 2)

Isotope	max(E_γ) (keV)	T_{max} (eV)
174	433	0.5
175	343	0.36
176	638	1.2
177	574	1.7
178	495	0.74
179	454	0.62
180	615	1.2
181	482	0.69

2.3. The displacement rate

The number of displaced atoms per time unit, K, induced by elastic collisions between neutrons and atoms and $^{10}B(n,\alpha)^7Li$ can be written as follows:

$$K = K^{el} + K^{ab},$$

where

$$K^{el} = \int_o^{E_n^{max}} F(E)\frac{\partial\phi(E_n)}{\partial E_n}\mathrm{d}E_n$$

and

$$F(E) = \sum_{i=1}^{p}\left[c_i\int\frac{\mathrm{d}\sigma_{ni}}{\mathrm{d}T}(E,T)P(T)\,\mathrm{d}T + \sum_{j=1}^{p}c_j\int\frac{\mathrm{d}\sigma_{nj}}{\mathrm{d}T}(E,T)n_{ji}(T)\,\mathrm{d}T\right],$$

where n_{ij} is obtained by the formalism described above. The first term in brackets of the equation expresses the number of displaced atoms by a neutron of energy E. Each atom displaced is a PKA and induced displacement cascades estimated by the second term of the equation and $\partial\phi(E_n)/\partial E_n$ is the neutron spectrum between 0 and E_n^{max}, and

$$K^{ab} = \int_0^{E_n^{max}}\left[c(^{10}B)\sigma^{ab}(E)\right]\frac{\partial\phi(E_n)}{\partial E_n}\mathrm{d}E_n.$$

$c(^{10}B)\sigma^{ab}(E)$ is the probability for a neutron to be captured by 10 boron atoms. This probability is equal to the $^{10}B(n,\alpha)^7Li$ cross-section multiplied by the probability of finding a 10 boron atom, which is equal to the atomic fraction of 10 boron $c(^{10}B)$.

3. Dpa calculations for absorbing materials

It is quite difficult to compare the calculated number of displaced atoms with experimental measurements. We have compared the number of displaced atoms due to the elastic scattering as calculated by DIANE to the ones obtained by the well-known code, TRIM-91. Both codes rely on the BCA scheme, and neglect the effect of the crystalline structure of the target.

Table 2
Comparison between DIANE and TRIM-91 of the number of displaced atoms created by an atom of Al on a target of Al

Energy (eV)	DIANE	TRIM-91
10^2	1.03	1
10^3	14.5	16
10^4	127	141
10^5	882	970
10^6	2701	3061
10^7	5555	4273

The threshold energy has been taken equal to 25 eV for Al.

3.1. Comparison between TRIM-91 and DIANE

In order to test the number of displaced atoms due to elastic collisions, we have first compared DIANE and TRIM-91 for several monoatomic targets. A very good agreement is found (see Table 2).

A similar work has been done on a polyatomic target, boron carbide, irradiated by ^{10}B. As TRIM-91 does not allow different threshold energies of elements in a compound, threshold energies are taken as 20 eV both for carbon and boron in both codes. The results are listed in Table 3.

The agreement is fair. Notice that at high energies, DIANE calculations give higher numbers of displaced atoms.

Therefore, DIANE can easily calculate dpa produced by nuclear reactions in materials, and also permits to choose a different value of the threshold energy for each species of atoms in the target.

3.2. Dpa calculations for boron carbide and hafnium diboride in a PWR neutron spectrum

DIANE has been used to calculate dpa induced by neutrons with an energy varying from 25 meV (thermal neutrons) to 10 MeV for boron carbide (Fig. 1) and hafnium diboride (Fig. 2). These calculations have been

Table 3
Comparison between DIANE and TRIM-91 of the number of displaced atoms created by an atom of bore on a target of boron carbide

Energy (eV)	DIANE	TRIM-91
10^4	348	349
10^5	619	545

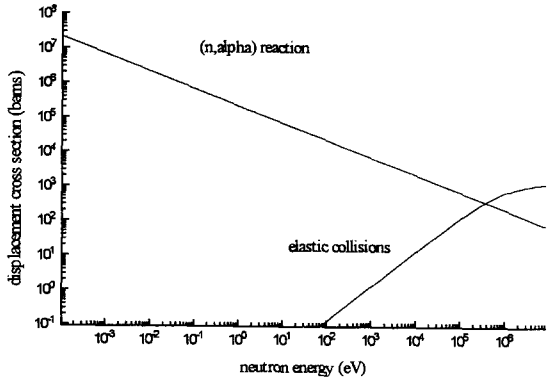

Fig. 1. Dpa created in a slide of non-depleted boron carbide for a fluence of 10^{28} n m^{-2} as a function of the neutron energy. At low neutron energies, dpa are produced by the $^{10}B(n,\alpha)^{7}Li$ reaction whereas at high neutron energies, dpa are produced by neutron atoms elastic collisions.

done with threshold energies of 20 eV for boron and carbon [15], and 50 eV for hafnium [16].

For low neutron energies (< 1 keV), all the dpa are created by the $^{10}B(n,\alpha)^{7}Li$ reaction. The effect of elastic collisions between neutrons and atoms of the lattice plays a role only for high neutron energies (1 MeV). The effect of recoil atoms produced by the $^{10}B(n,\alpha)^{7}Li$ reaction is of the same order of magnitude as the effect due to neutron collisions for a typical PWR neutron spectrum.

During the neutron irradiation, ^{10}B atoms are transmuted into lithium and helium atoms with different masses and different threshold energies. The decrease in ^{10}B atomic fraction modifies the displacement rate of the absorber.

Fig. 3 shows how the dpa due to a neutron irradiation depend on the irradiation fluence. The dpa decrease as the fluence increases especially for low neutron energies. For

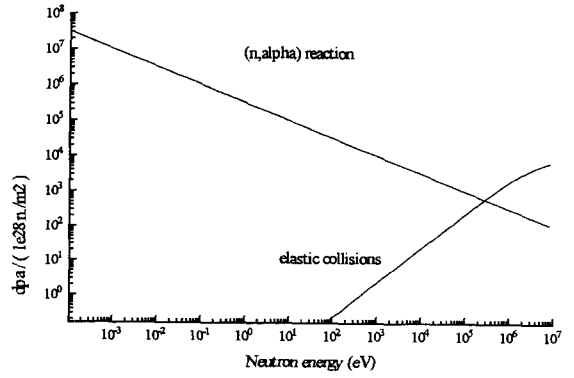

Fig. 2. Dpa created in a slide of non-depleted hafnium diboride for a fluence of 10^{28} n m^{-2} as a function of the neutron energy. At low neutron energies, dpa are produced by the $^{10}B(n,\alpha)^{7}Li$ reaction whereas at high neutron energies, dpa are produced by neutron atoms elastic collisions.

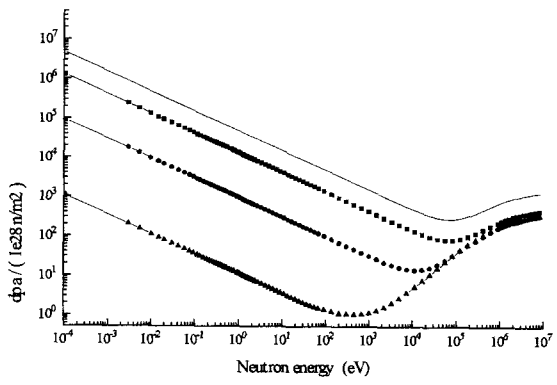

Fig. 3. Dpa produced in a slide of boron carbide pellet for different fluences as a function of the neutron energy. When fluences increase, the ^{10}B atomic fraction and then the dpa due to the $^{10}B(n,\alpha)^{7}Li$ reaction decrease. Moreover, the minimum of the dpa curves is shifted to low neutron energies. This shift is due to the chemical modification (transformation of ^{10}B atoms in lighter elements ^{7}Li and ^{4}He) of the target. ————: 0 n cm^{-2}; ■: 2.1×10^{20} n cm^{-2}; ●: 1.3×10^{21} n cm^{-2}; △: 2.5×10^{22} n cm^{-2}.

low neutron energies, dpa are essentially due to the recoils produced by the $^{10}B(n,\alpha)^{7}Li$ reaction and then to the ^{10}B atomic fraction. This ^{10}B atomic fraction decreases because the $^{10}B(n,\alpha)^{7}Li$ is more efficient for low neutron energies. If we assume that the material remains homogeneous and exposed to neutron fluxes, these dpa are largely reduced when the fluence becomes important (see Fig. 3). Moreover, the modification of the boron carbide composition does not modify the number of dpa due to elastic collisions between neutrons and atoms.

4. Geometrical effects in absorber pellets

It has been shown that dpa depend on the fluence irradiation in an boron carbide and hafnium diborides pellets.

In order to determine dpa along the radius of a pellet during a neutron irradiation, the self-shielding of ^{10}B must be taken into account. The high absorbing cross-section of ^{10}B modifies the neutron energy spectrum of thermal and epithermal neutrons in the absorber, and then modifies the ^{10}B atomic fraction in the absorber by a feedback effect. This effect is responsible for the non-uniform ^{10}B, ^{7}Li and ^{4}He atomic fraction distribution along the radius of the absorbing pellet during a neutron irradiation.

4.1. Dpa calculations as a function of the radial distance

Before an irradiation, the atomic fraction of ^{10}B is uniform inside the absorbing pellet. During the neutron irradiation, ^{10}B atoms absorbing neutrons are destroyed and a ^{10}B atomic fraction distribution along the radius of

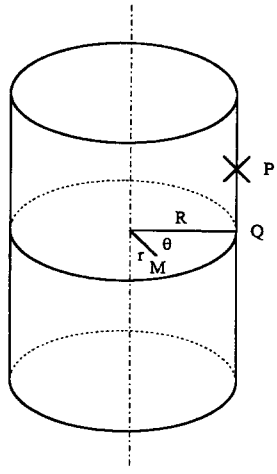

Fig. 4. Schema of a cylindrical absorbing pellet. Point P is a point of the pellet surface, Q is the projection of point P in the plain containing point M (r, θ). R is the radius of the pellet.

the pellet appears. The mean free path of a neutron with the energy E_n is $1/(N(^{10}B)\sigma(E_n))$. This mean free path is very small in the absorber. Neutrons do not scatter and do not go through the absorber. That is why the neutron spectrum decreases near and inside the absorber. The diminution of the neutron spectrum is quantified by a form factor. It is possible to define a neutron spectrum form factor inside the absorbing pellet by

$$f(r, E, t) = \frac{\partial\phi(r, E, t)/\partial E}{\partial\phi_{np}(r, E, t)/\partial E} = \frac{1}{4\pi}\int\int_{4\pi}\exp\left(-\int_0^1\left(\sum_{i=1}^{p} N_i(\mathrm{P}+\mu\mathrm{PM}, t)\times\sigma_i\|\mathrm{PM}\|\,\mathrm{d}\mu\right)\right)\mathrm{d}\Omega, \quad (6)$$

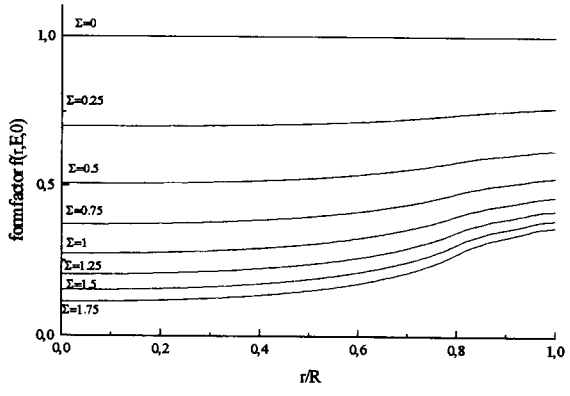

Fig. 5. The form factor $f(r, E, t)$ defined in Eq. (7) can be easily expressed for $t = 0$. Noticing Σ the term $R\Sigma_{i=1}^{p} N_i(t=0)\sigma_i(E)$ and $x = r/R$, the form factor can be expressed as a function of x for different values of Σ.

Table 4
The $^{10}B(n,\alpha)^7Li$ reaction generates ^7Li and ^4He atoms. The high energies of these recoils (0.83 MeV for ^7Li and 1.48 MeV for ^4He) generate a number of displaced atoms in boron carbide and hafnium diborides absorbers

Projectiles	Total number of displaced atoms, n, in B_4C	Total number of displaced atoms, n, in HfB_2
^7Li (0.83 MeV)	259	327
^4He (1.43 MeV)	106	174

where N_i is number of absorbing atoms per volume through the path PM and at the time t, and $\sigma_i(E_n)$ is the neutron absorbing cross-section of the ith species in the material. $\partial\phi_{np}(r, E, t)/\partial E$ is the neutron spectrum out of the pellet which is here considered as isotrope.

After tedious calculations, $f(r, E, t)$ can be expressed in a cylindrical pellet by the following expression:

$$f(r, E, t) = \frac{1}{\pi}\int_0^{\pi}\frac{(1-(r/R)\cos\theta)}{(1-2(r/R)\cos\theta+(r/R)^2)} \times Ki_2\left(-R\sqrt{1+\left(\frac{r}{R}\right)^2-2\left(\frac{r}{R}\right)\cos\theta} \times\int_0^1\left(\sum_{i=1}^{p} N_i(\mathrm{Q}+\mu\mathbf{QM}, t)\sigma_i(E)\,\mathrm{d}\mu\right)\right)\mathrm{d}\theta, \quad (7)$$

where R is the pellet radius, Ki_2 is the second order modified Bessel function. P, M and Q are defined in Fig. 4. $f(r, E, t)$ depends on t because the number of atoms i per volume unit along the line QM decreases in time. Knowing $f(r, E, t)$ thanks to Eq. (7) permits to calculate the burnup rate of the atoms i and then the number of i atoms at the position r and at the time t in the pellet. Fig. 5 shows the form of $f(r, E, 0)$.

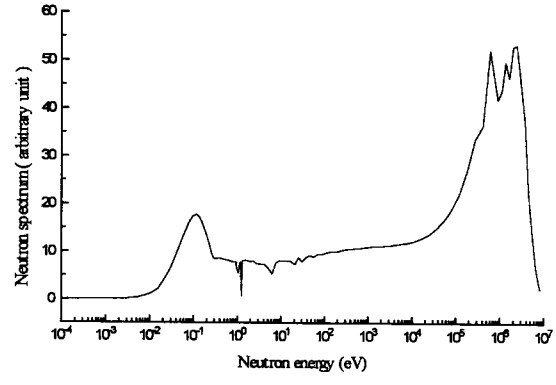

Fig. 6. Typical neutron PWR spectrum (enrichment: 3.7% in $^{235}_{92}U$; burnup 12 GWd/t for 280 days, 103 tons of uranium and a fission mean energy of 200 MeV, i.e., 1.38×10^{20} fissions/cm^3).

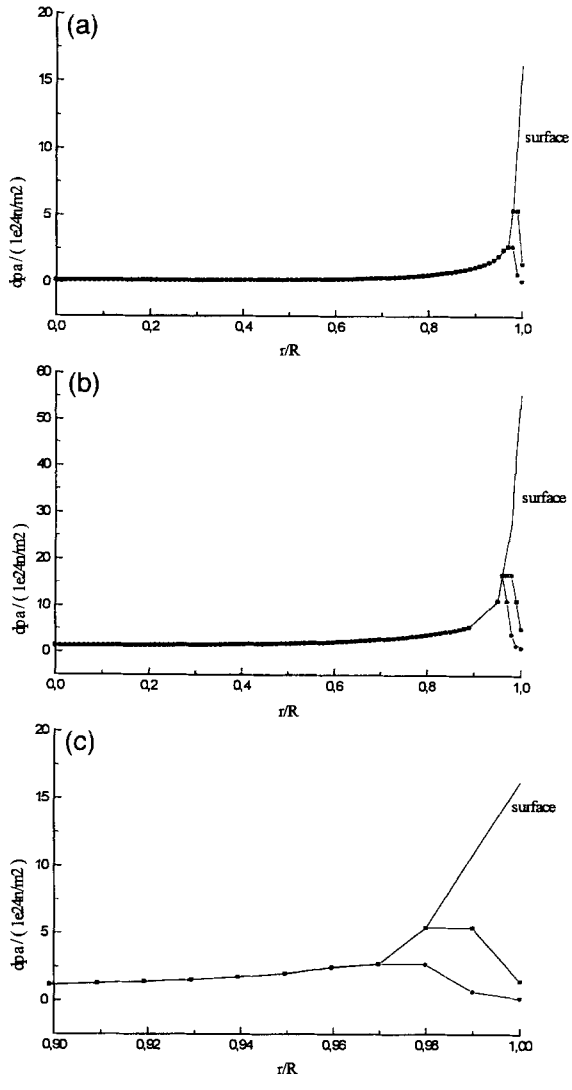

Fig. 7. (a) Dpa as a function of the reduced abscissa ($R = 3.35$ mm) for a non-depleted boron carbide pellet at different fluences. The dpa peak is shifted to the center of the pellet when the fluence increases. The ^{10}B atoms are burned from the surface to the center and then the maximum of dpa curves goes inward towards the pellet when the fluence increases. Besides, the background of the dpa curves along the pellet radius is constant and due to neutron atoms elastic collisions. (b) Dpa as a function of the reduced abscissa ($R = 3.35$ mm) for a non-depleted hafnium diboride pellet at different fluences. The dpa peak is shifted to the center of the pellet when the fluence increases. As hafnium atoms have a heavier mass than carbon ones, the dpa background is more important than in (a). (c) Dpa as a function of the reduced abscissa for a non-depleted boron carbide pellet for different fluences. The form of the dpa maxima of the curves is sharp. These sharp peak are due to the ^{10}B high absorption cross-section for thermal neutrons. ————: 0 n cm^{-2}; ■: 1.3×10^{21} n cm^{-2}; ●: 2.5×10^{22} n cm^{-2}.

A specific code has been developed to estimate the neutron flux distortion induced by the absorber inside an absorbing pellet. This code has been used to calculate the number of ^{10}B atoms present at a time t along the radius of the pellet Table 4. If the number of ^{10}B atoms destroyed in the pellet is not too important, for instance $2\cdot10^{21}$ atoms per cm^3, i.e., a decrease of 2% in atomic fraction of ^{10}B, the dpa due to elastic collisions between neutrons and atoms will not vary much. These dpa curves have been fitted from the curves presented in Section 3 (Figs. 1 and 2) and added to the ^{10}B atomic fraction profile obtained by taking into account the self-shielding, to obtain the damage rate along the radius of an absorbing material:

$$K(r,t) = \int_0^{E_n^{max}} \left[F(E) + c(^{10}B, r, t)\sigma^{ab}(E) \right] \times f(r,t,E)\frac{\partial\phi_{np}(E)}{\partial E}\,dE, \quad (8)$$

where $f(r, t, E)$ is the form factor induced by the ^{10}B self-shielding for the boron carbide and by the hafnium isotopes for the hafnium diboride on the neutron spectrum inside the pellet.

For a typical PWR neutron spectrum (Fig. 6), dpa profiles have been calculated using Eq. (8) for boron carbide (Fig. 7a) and hafnium diboride (Fig. 7b). As expected, the dpa are high at the periphery of the pellet. A remarkable fact is that the dpa go through a maximum and that this maximum is moving inwards as ^{10}B is transmuted. A related phenomenon is that dpa curves as a function of the radius are not smooth around their maxima.

For a natural boron carbide irradiated in a PWR, some microcracks have been observed in transmitted electron microscopy [17]. On Fig. 4c, a zoom near the surface of the pellet has been done on dpa calculated curves. The maxima of the dpa for $13\cdot10^{21}$ and $25\cdot10^{21}$ n m^{-2} are at the reduced abscissa of 0.98. The maximum microcracks density for similar fluences and similar pellets observed on photographs is near the maximum of the dpa obtained in our calculations. This maximum dpa also coincides with a maximum in the production rate of helium. The effects of the damage rate and of the helium production rate may play a cumulative role in the creation of microcracks.

Table 5
Comparison of the dpa/n m^{-2} induced by recoil atoms and elastic neutron atom collisions in a boron carbide pellet during a PWR irradiation. This table shows that dpa induced by recoils are predominant

Fluence ($\times10^{20}$ n cm^{-2})	0	13	250
Damage per 10^{24} n m^{-2} due to recoils (%)	0.89	0.85	0.83
Damage per 10^{24} n m^{-2} due to neutron scattering (%)	0.11	0.15	0.17
Total damage per 10^{24} n m^{-2}	3.29	2.49	1.98

Table 6
Comparison of the dpa/nm^{-2} induced by recoil atoms and elastic neutron atom collisions in an hafnium diboride pellet during a PWR irradiation

Fluence ($\times 10^{20}$ n cm^{-2})	0	13	250
Damage per 10^{24} n m^{-2} due to recoils (%)	0.82	0.77	0.72
Damage per 10^{24} n m^{-2} due to neutron scattering (%)	0.18	0.23	0.28
Total damage per 10^{24} n m^{-2}	15.75	11.07	9.25

The number of dpa induced by the $^{10}B(n,\alpha)^7Li$ is less important than in Table 5 because the ^{10}B atomic fraction in HfB_2 is lower than the ^{10}B atomic fraction in B_4C. Moreover, as the hafnium mass is heavier than the carbon one, dpa due to the neutron atom collision are more important. An important fact to notice is that the majority of dpa is produced by the $^{10}B(n,\alpha)^7Li$ reaction as in boron carbide.

4.2. Role of recoil atoms in the displacement rate in an pellet

Calculations have been done to estimate dpa due to helium and lithium recoils and elastic interactions between neutrons and lattice atoms. The results of these calculations are given in Tables 5 and 6.

The important result is that, for a PWR neutron spectrum, the major part of radiation damage is due to recoils of atoms created during the nuclear reaction $^{10}B(n,\alpha)^7Li$. In metallic targets, it is known that damage calculations using the BCA overestimate the number of defects really created, since at the end of the lifetime of displacement cascades, many-body interactions result in the recombination of an important fraction of the defects initially created in the so-called collisional phase of the displacement cascade [5,6]. The fraction of defects surviving this annealing stage decreases with increasing PKA energy, but also seems to depend on the compactness of the structure (less isolated defects would survive in close-packed structures). In non-metallic targets, the understanding of this dynamic recovery is far less advanced, and is mostly restricted to silicon. For this material, only short replacement collision sequences can take place because of the difficulty to focus the kinetic energy along atomic rows. As a result, few defects are expected to survive at the end of the cascade. Some recent molecular dynamics (MD) simulations [18] tend to suggest that for low mass PKA, the fraction of isolated defects which will survive after the cascade in Si may be about one third of the value expected from the BCA. This implies that the contribution of Li and He recoils to radiation damage in absorbing materials is not as overwhelming as what is calculated in this paper (Tables 5 and 6). Indeed, Li and He recoils lead to more energetic cascades than collisions produced by the elastic scattering of neutrons, and should therefore be more affected by the intracascade recombination. However, it remains true that recoils from nuclear reactions account for an important part of the radiation damage in these materials. More accurate numbers will be obtained when MD simulations will be performed, which implies first that reliable interatomic potentials have to be developed for such absorbing materials. Notice that efficiency factors can be incorporated in DIANE, as soon as this information will become available.

5. Conclusion

In this paper, we used a model developed by Lesueur and neutronic calculations to estimate the dpa along the radius of absorbing materials. Our neutronic calculations permit to obtain dpa along the radius of the pellet at different neutron fluxes for a typical PWR neutron spectrum. It is shown that for both boron carbide and hafnium diboride (a new candidate for absorber pellets) a large fraction of the damage produced under reactor conditions results from the ^7Li and ^4He recoils due to ^{10}B transmutation. Furthermore, the calculated dpa curves exhibit a sharp maximum which moves towards the centre of the pellet as the burnup of ^{10}B increases. This is a direct consequence of the ^{10}B self-shielding effect. We hope the quantitative results presented in this paper will stimulate the study of radiation damage in absorbing materials. The interest of our calculation is to calculate dpa along the radius of the pellet which can be used to define a defects production rate in rate equations which control the microstructural evolution of such materials.

Acknowledgements

The authors gratefully thank Mr D. Lesueur for helpful discussions. Without his work on defects induced by irradiation in polyatomic targets, our calculations on absorbing materials would have never been done.

References

[1] T. Stoto, L. Zuppiroli, J. Pellissier, Radiat. Eff. 90 (1985) 160.
[2] A. Albermann, D. Lesueur, Am. Soc. for Test. and Mat., PA 19103, 1989.
[3] J. Ziegler, J. Biersack, U. Littmark, The Stopping Power and Range of Ions in Solids, Vol. 1 (Pergamon, Oxford, 1985).
[4] M.J. Norgett, M.T. Robinson, I.M. Torrens, CEA Report CEA-R-4389, 1972.
[5] D.J. Bacon, T. Diaz De La Rubbia, J. Nucl. Mater. 216 (1994) 275.
[6] N.V. Doan, F. Rossi, Solid States Phenom. 30&31 (1993) 75.
[7] J. Lindhart, V. Nielsen, M. Scharff, Mat. Fys. Medd. Dan. Vid. Selsk. 36 (1968) 1.
[8] J. Lindhart, Phys. Rev. B14 (1961) 1.

[9] H. Bethe, R.W. Jackiw, Intermediate Quantum Mechanics, 2nd Ed. (W.A. Benjamin, New York, 1968) p. 302.
[10] J. Ziegler, Nucl. Instrum. Methods 169 (1980) 77.
[11] G. Kinchin, R. Pease, Rep. Prog. Phys. 18 (1955) 1.
[12] W.E. Meyerhof, Element of Nuclear Physic (Dunod, 1970) p. 217.
[13] J.R. Stehn, M.D. Goldberg, B.A. Magurno, R. Wiener-Chasman, Neutron Cross Section, B.N.L. 325, Vol. 1, 1964, p. 5-10-3.
[14] R. Pannetier, Vade Mecum du Technicien Nucleaire, Vol. 2, 1980, p. 433.
[15] L. Zuppiroli, R. Kormann, D. Lesueur, CEA Report CEA-R-5237, 1983, p. 39.
[16] D. Simeone, work in progress.
[17] EPRI, Control Rod Materials and Burnable Poisons, Contract TPS 79-708, NP, 1974, p. 479.
[18] T. Diaz de la Rubia, Ann. Rev. Mater. Sci. 26 (1996) 613.